Electronic Supplementary Information for

Enhancing the Intermolecular Singlet Fission Efficiency by Controlling Self-assembly of Amphipathic Tetracene Derivatives in Aqueous Solution

Zhaofeng Tang, Sainan Zhou, Xiangyang Wang, Heyuan Liu*, Xinyu Yan, Shanshan Liu, Xiaoqing Lu, and Xiyou Li*

School of Materials Science and Engineering, Institute of New Energy, College of Science, China University of Petroleum (East China), Qingdao, Shandong, 266580, China.
E-mail:xiyouli@upc.edu.cn.

Contents

1. Experimental Section 3
2. Simplified Crystal packing diagram of molecular PhTc-COOH 7
3. Simplified Crystal packing diagram of molecular PhTc 8
4. Crystallographic parameters for molecular PhTc-COOH and PhTc crystals 9
5. Triplet sensitization 10
6. TA measurements of triplet sensitization of PhTc suspensions following excitation of PtOEP at 355 nm. 11
7. TA measurements and the single-wavelength dynamics of triplet sensitization of PhTc-COOH NPs suspensions following excitation of PtOEP at 355 nm 12
8. Comparison of the triplet spectra between the sensitization experiment and SF for PhTc-COOHNPs and PhTc NPs 13
9. Comparison of TA spectra of PhTc-COOH NPs between the raw data and the fitting data in a three-component model obtained from the global method. 14
10. Comparison of Single-wavelength dynamics of PhTc-COOH NPs between the raw data and the fitting data in a three-component model obtained from the global method 15
11. Comparison of the spectrum of the third component and the T1state obtained from the sensitization experiment in PhTc-COOH NPs. 16
12. Comparison of TA spectra and single-wavelength dynamics of PhTc NPs between the raw data and the fitting data with a three-component model obtained from the global analysis 17
13. Comparison of TA spectra of PhTc NPs between the raw data and the fitting data in a four-component model obtained from the global analysis 18
14. Comparison of single-wavelength dynamics of PhTc-COOH NPs between the raw data and the fitting data in a four-component model obtained from the global analysis. 19
15. Triplet yield determination 20
16. The ^{1}H NMR spectrum of compound PhTc-COOH. 22
17. The MALDI-TOF spectrum of compound PhTc-COOH. 23
REFERENCES 23

1. Experimental Section

1.1 General Methods

^{1}H NMR spectra were recorded on a Bruker 400 MHz NMR spectrometer with chemical shifts reported in ppm (TMS as internal standard). MALDI-TOF mass spectra were recorded with a Bruker/ultraflex instrument. Absorption spectra were measured on Hitachi U-9300 spectrophotometer. Steady-state fluorescence spectra were recorded on an Edinburgh Instruments FLS980 with three-monochromator spectrophotometer and three photomultiplier detectors. The emission spectra were corrected for the wavelength dependence of the sensitivity of the detection system. The fluorescence lifetimes were measured on FLS980 with timecorrelated single photon counting (TCSPC) method by excitation with a 441 nm picosecond laser (EPL 445). Time resolution for time resolved fluorescence spectrum is 50 ps. The absolute fluorescence quantum yields were measured with an integrating sphere. All samples used for the photophysical measurement was prepared in glovebox. The path-length of the cuvette used for collecting absorption and fluorescence spectra is 1 cm. All the solvents used for preparing the solutions for photophysical measurement were degassed first by Freeze-Pump-Thaw method prior to use.

1.2 Femtosecond transient absorption spectroscopy

For ultrafast femtosecond transient absorption (fsTA) spectroscopy, the pump beam was set at 450 nm that was generated from a regeneratively amplified Ti: sapphire laser system (Coherent, 800 nm, 100fs, 6 mJ/pulse, 1kHz) pumped TOPAS system (Light Conversion). A small portion of the amplifier out was used to generate the super continuum white light probe which was delayed with respect to pump pulse with an optical delay line. The pump spot diameter was set to 0.6 mm with per-pulse energies of 17.7 μJ/cm^2. The pump pulse was kept in a weak regime where the

excitonic annihilation effect can be neglected. Nanoparticle suspensions were prepared fresh prior to *fs*-TA experiments and were excited at 450 nm in a 2 mm path length cuvette.

1.3. Materials

Tetracene, 4-carboxyphenylboronic acid, phenylboronic acid were purchased from TCI or Aldrich. Solvents were of analytical grades. 5-bromotetracene and5-phenyltetracene (PhTc) were synthesized following the method reported in previous literatures.[1,2]

1.3.1 Synthesis of PhTc-COOH:

A mixture of 5-bromotetracene (153 mg, 0.5 mmol), 4-carboxyphenylboronic acid (83.0 mg, 0.5 mmol), $Pd(PPh_3)_4$ (57.8 mg, 0.05 mmol), and K_2CO_3 (691 mg, 5 mmol) in a dried round bottom flask was subjected to sequential vacuum and argon to degas the reaction mixture. Then degassed 1,4-*dioxane* (40 mL) and H_2O (10 mL) were added. The resulting solution was heated to 90℃ and maintained at this temperature for 18h in dark. After the mixture was cooled to room temperature, the mixture was acidized with HCl (2M). The solution was then transferred into a separatory funnel containing dichloromethane (50 mL) and water (100 mL). The organic layer was separated, and dried over anhydrous $MgSO_4$for overnight. The liquid was separated by filtration and then removed under reduced pressure. The resulting crude product was purified by column chromatography on silica gel (dichloromethane/methanol = 14/1), A red solid was obtained (248.5 mg, 72% yield).^{1}H NMR (400 MHz, DMSO-d_6, δ): 13.16 (s 1H, O H), 8.97 (s, 1H, Ar H), 8.92 (s, 1H, Ar H), 8.26 (d, J = 8 Hz, 2H; Ar H), 8.18 (d, J = 9.1 Hz, 2H; Ar H), 8.11 (d, J = 8.6 Hz, 1H; Ar H), 7.92 (d, J = 8.6 Hz; 1H, Ar H), 7.64 (d, J = 8.0 Hz, 2H; Ar H), 7.47(dd, J = 14.0 Hz, 3H; Ar H), 7.39 (dd, J = 14.0 Hz, 2H; Ar H). MALDI-TOF: m/z: calculated: 349.41 $[M+H]^+$; found:

349.06 $[M+H]^+$; elemental analysis (%), calculated for $C_{25}H_{16}O_2$: C 86.19, H 4.63, O 9.18; found: C 86.22, H 4.51, O 9.27.

1.3.2 Nanoparticle preparation

NPs were prepared by the re-precipitation method[3,4] in which a solution of PhTc-COOH or PhTc in THF (0.2ml) at aconcentration of 5mM is added to a vigorously stirred deionized water (10 mL). The solutions were stirred for 3h to give orange (PhTc-COOHNP) or yellow (PhTc NP) solution of NPs suspended in water. All the aqueous nanoparticle suspensionswere prepared in glovebox and all the solvents are degassed first by Freeze-Pump-Thaw method. Concentrated aqueous nanoparticle suspensions were passed through a 2 μm pore size syringe filter before measurements. Sample suspensions were stored indark in glovebox to avoid photo-oxidation.

1.4. Crystal structure determinations

Single crystal of PhTc wasgrown by recrystallization from dichloromethane and methanol (dichloromethane/methanol = 5:1) while single crystal of PhTc-COOH recrystallization from dichloromethane and n-Hexane (dichloromethane/n-Hexane= 1:4). These single crystals were reported in this article for the first time. The crystallographic data of PhTc and PhTc-COOH ware collected on the Agilent Xcalibur Eos Gemini diffractometer with (Cu) X-ray Source (Cu-Kα λ = 1.54184 Å). Experienced absorption was corrected by multiscan method. Using the SADABS program to apply the empirical absorption correction.[5] The structures were solved by the direct method and refined by the full-matrix least-squares method on F2, and all non-hydrogen atoms are refined with anisotropic thermal parameters.[6] The structures of PhTc-COOH and PhTc have been deposited in the Cambridge Crystallographic Data Centre database (CCDC 1892455 for PhTc-

COOH, 1892456 for PhTc). All the cell parameters and refinement details were given in the Supporting Information (Table S1).

1.5. Powder XRD

Powder X-ray diffraction (XRD) patterns were recorded by an Rigaka Ultima IV diffractometer operating at 40 mA and 40 kV, by using the Cu Ka irradiation (wavelength=0.1538 nm). Nanoparticle samples for XRD were prepared by concentrating the aqueous colloidal nanoparticles suspensions and subsequently dehydrating the suspension through freeze drying. Bragg angles are scanned between 5° and 50° with a scan rate of 20°/min and step of 0.028°/2.

1.6. Scanning electron microscope (SEM)

SEM samples were prepared by dropping the suspension on a silicon wafer and then dried at 80℃. SEM images were recorded by using a JEOL JSM-6700F microscope at an accelerating voltage of 5 kV.

2. Simplified Crystal packing diagram of molecular PhTc-COOH

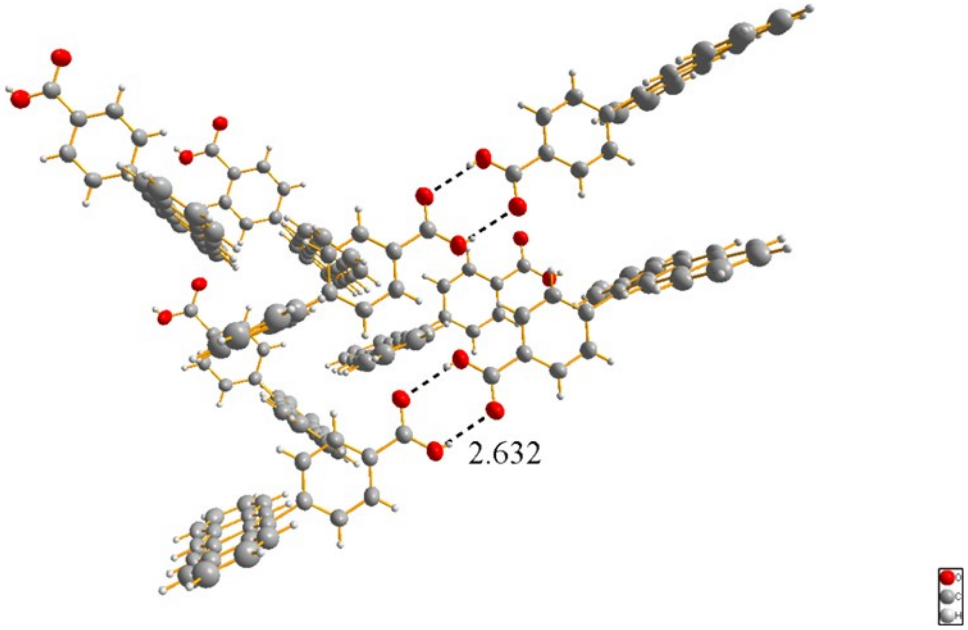

Fig. S1 Simplified Crystal packing diagram of molecular PhTc-COOH. The length of hydrogen bond is 2.632 Å.

3. Simplified Crystal packing diagram of molecular PhTc

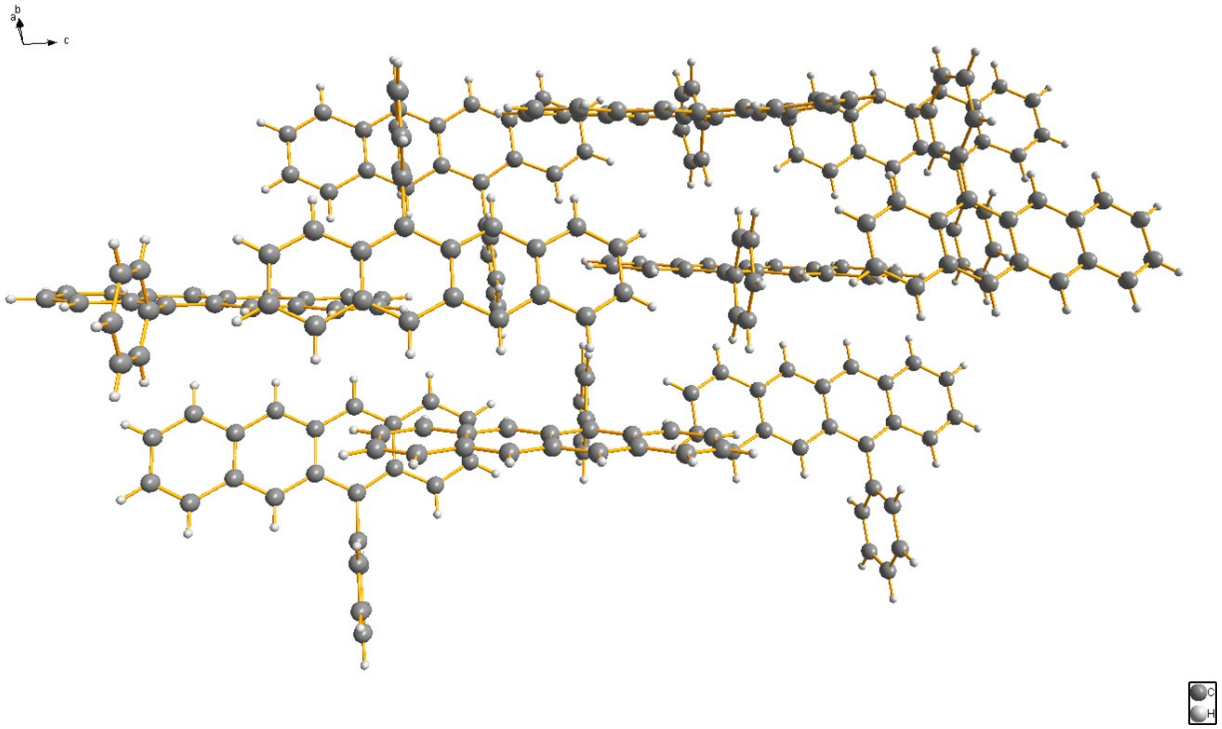

Fig. S2 Simplified Crystal packing diagram of molecular PhTc.

4. Crystallographic parameters for molecular PhTc-COOH and PhTc crystals

Table S1. Crystallographic parameters for molecular PhTc-COOH and PhTc crystals.

	PhTc-COOH	PhTc
Empirical	$C_{25}H_{16}O_2 \cdot CH_2Cl_2$	$C_{24}H_{16}$
Formula	429.11	304.13
Temperature/K	293.2(2)	150.00(10)
Crystal	monoclinic	triclinic
Space	$P2_1/c$	p-1
a/Å	9.1718(3)	13.3341(14)
b/Å	7.4763(2)	14.3315(16)
c/Å	30.5830(9)	17.3246(17)
α/°	90	101.642(9)
β/°	91.843(3)	90.149(8)
γ/°	90	90.054(9)
Volume/Å3	2114.51(50)	3242.6(6)
Z	4	2
ρcalc mg/mm3	1.348	1.247
μ/mm^{-1}	1.322	0.071
F(000)	857	1280.0
2Θ range for data collection	9.648 to 141.08	3.368 to 51.6
Reflections collected	7923	13311
Independent reflections	3923 [R_{int} = 0.0136, R_{sigma} = 0.0186]	9345 [R_{int} = 0.0535, R_{sigma} = 0.1075]
Data/restraints/parameters	3923/0/275	9345/0/385
Goodness-of-fit on F^2	1.330	1.048
Final R indexes [I>=2σ (I)]	R_1 = 0.0921, wR_2 = 0.2998	R_1 = 0.1004, wR_2 = 0.2435
Final R indexes [all data]	R_1 = 0.1045, wR_2 = 0.3262	R_1 = 0.1871, wR_2 = 0.3185
Largest diff. peak/hole /e Å-	0.54/-0.60	0.58/-0.28

5. Triplet sensitization

To obtain the triplet spectral signature of PhTc-COOH and PhTc NPs, triplet sensitization of PhTc-COOH and PhTc suspensions was performed with the known triplet sensitizer, platinumoctaethylporphyrin (PtOEP). The triplet sensitization NP sample were prepared by adding0.4 mL THF solution of 0.304 mg of PhTc or 0.35 mg PhTc-COOH and 0.0295mg of PtOEP to a vigorously stirred deionized water (10 mL). The triplet sensitization sample is prepared in glovebox and all the solvents are degassed first by Freeze-Pump-Thaw method. Photoexcitation of the PtOEP excited at 355 nm results in rapid intersystem crossing followed by triplet energy transfer to PhTc or PhTc-COOH (Figure S3 and S4). At initial times, there are the clear spectral signature observed corresponds to the reported T_1-T_n absorption (425 nm) and the ground-state bleaching (GSB) (539 nm) of PtOEP (Figure S3 and S4).[7,8] As the time delay, the triplet absorption of PtOEP centered at 425 nm decayed almost completely in hundred picoseconds (Figure S4B). Meanwhile, the GSB band of PtOEP was also decreased significantly. Anew spectrum with the main absorption band at 490 nm emerges, which can be assigned to the T_1 state of phenyl substituted tetracene based on the previous report.[9-11]

6. TA measurements of triplet sensitization of PhTc suspensions following excitation of PtOEP at 355 nm.

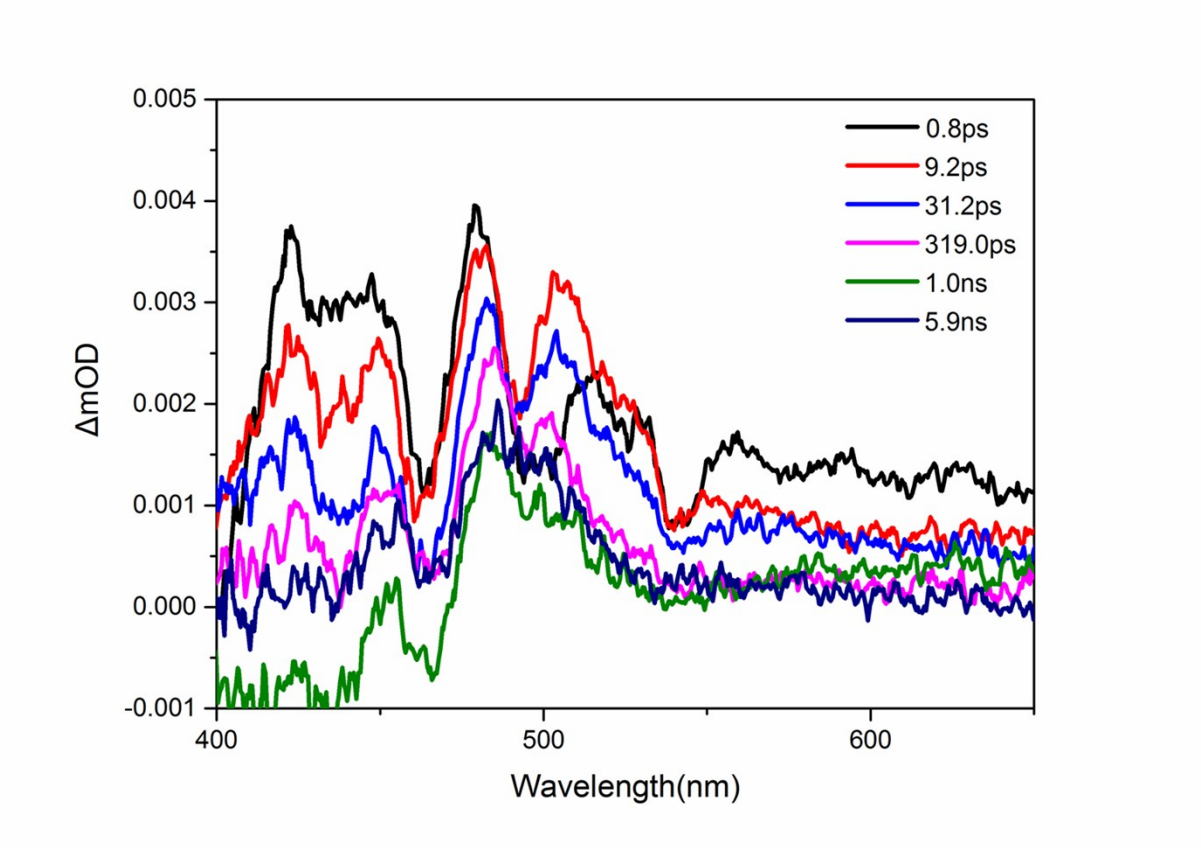

Fig. S3 TA measurements of triplet sensitization of PhTc suspensions following excitation of PtOEP at 355 nm.

7. TA measurements and the single-wavelength dynamics of triplet sensitization of PhTc-COOH NPs suspensions following excitation of PtOEP at 355 nm

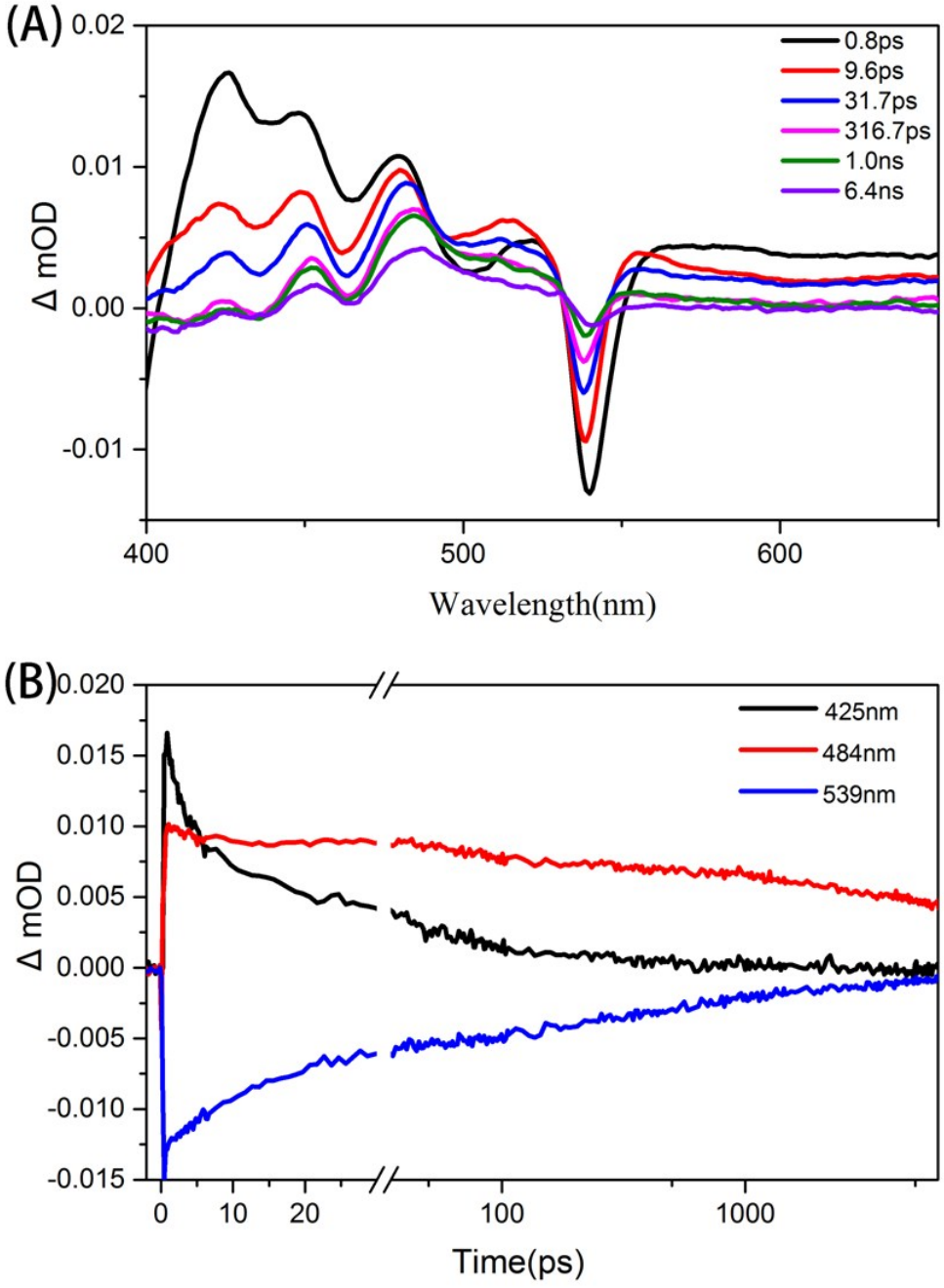

Fig. S4 (A) TA measurements of triplet sensitization of PhTc-COOH NPs suspensions following excitation of PtOEP at 355 nm. (B)The single-wavelength dynamics of PhTc-COOH NPs probed at different wavelengths.

8. Comparison of the triplet spectra between the sensitization experiment and SF for PhTc-COOHNPs and PhTc NPs

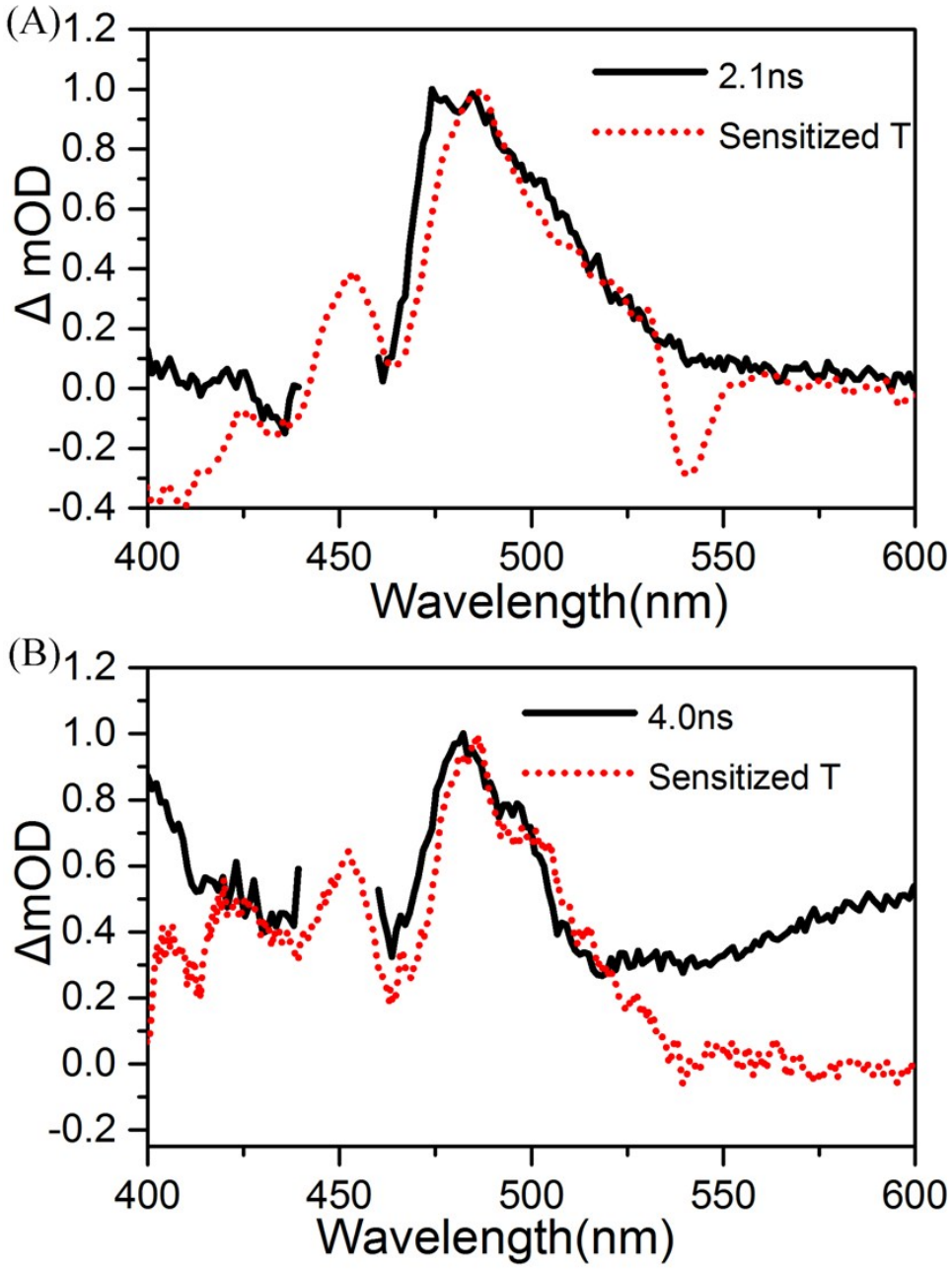

Fig. S5 Comparison of the triplet spectra between the sensitization experiment and SF for PhTc-COOHNPs (A) and PhTc NPs (B)

9. Comparison of TA spectra of PhTc-COOH NPs between the raw data and the fitting data in a three-component model obtained from the global method.

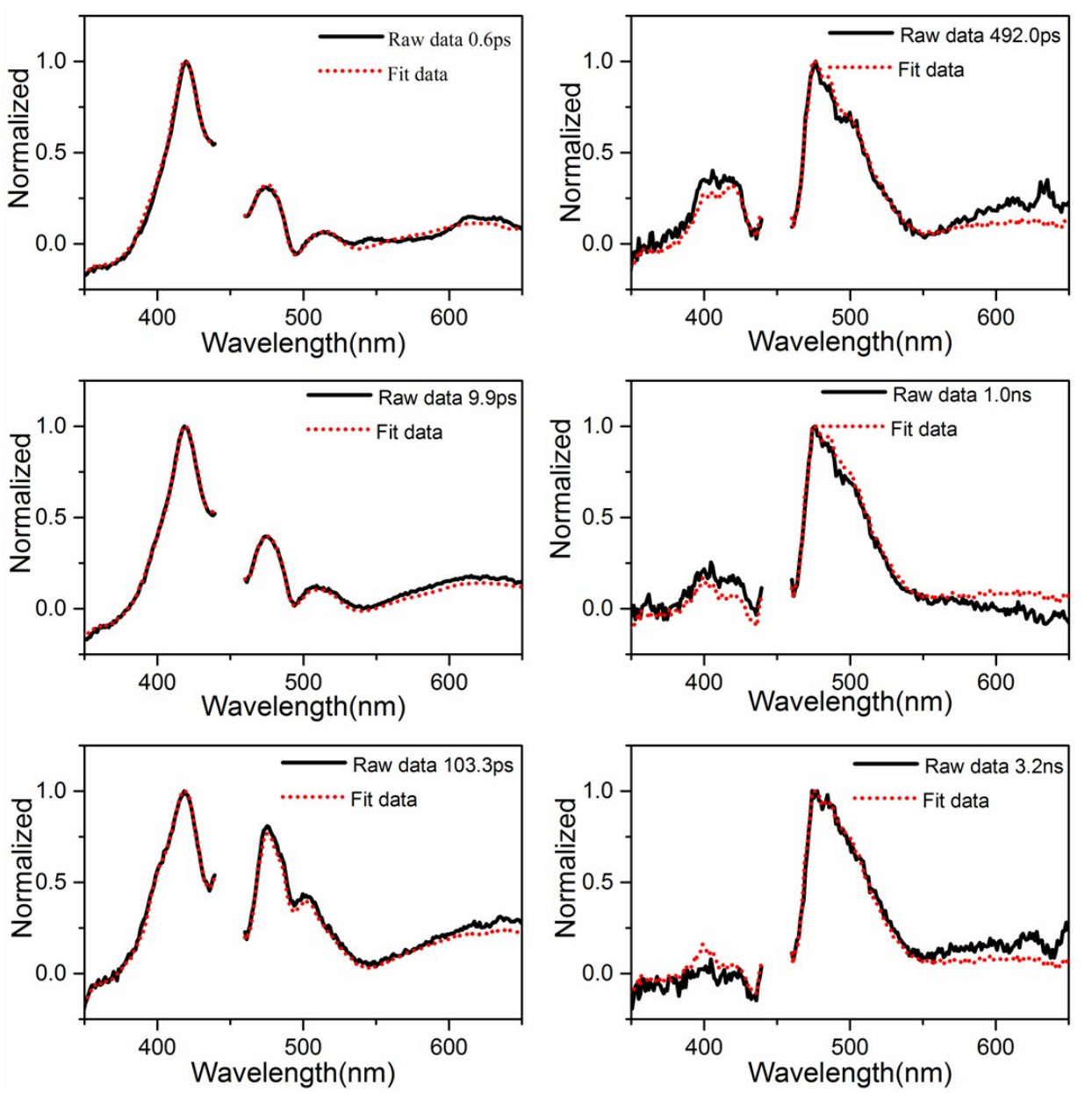

Fig. S6 Comparison of TA spectra of PhTc-COOH NPs between the raw data and the fitting data in a three-component model obtained from the global method.

10. Comparison of Single-wavelength dynamics of PhTc-COOH NPs between the raw data and the fitting data in a three-component model obtained from the global method

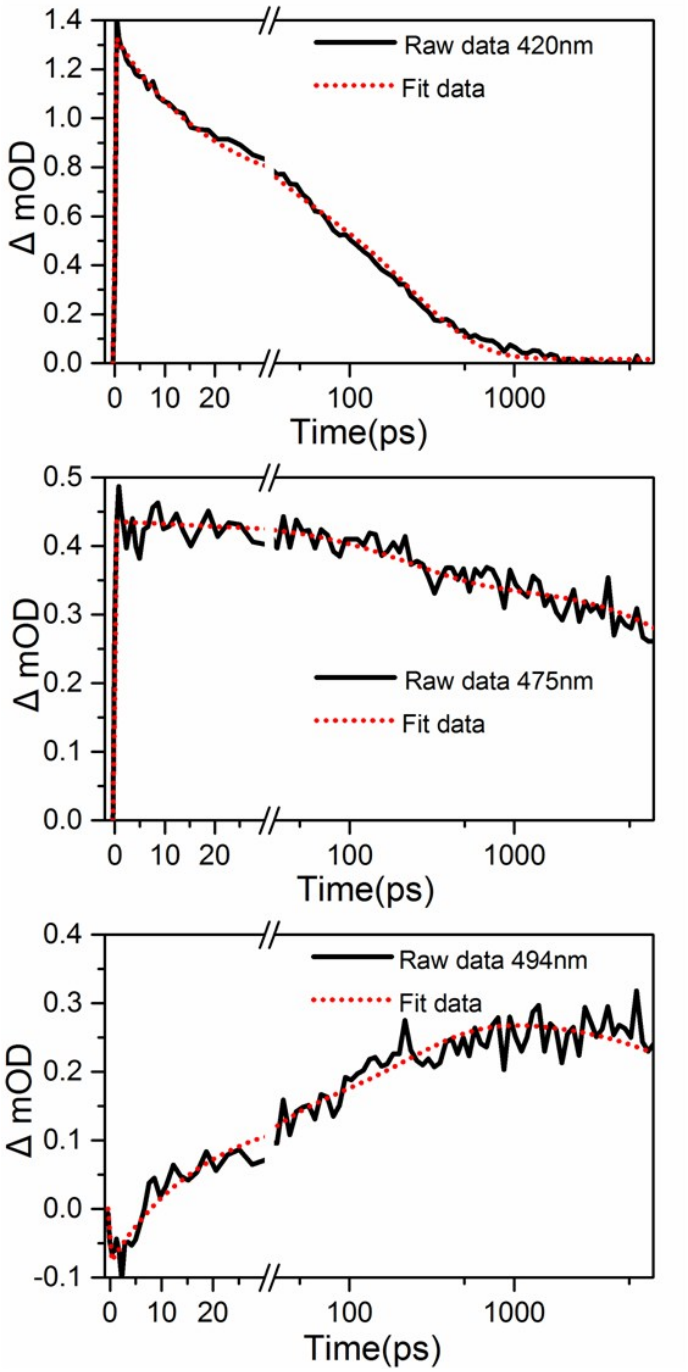

Fig. S7 Comparison of Single-wavelength dynamics of PhTc-COOH NPs between the raw data and the fitting data in a three-component model obtained from the global method.

11. Comparison of the spectrum of the third component and the T1state obtained from the sensitization experiment in PhTc-COOH NPs.

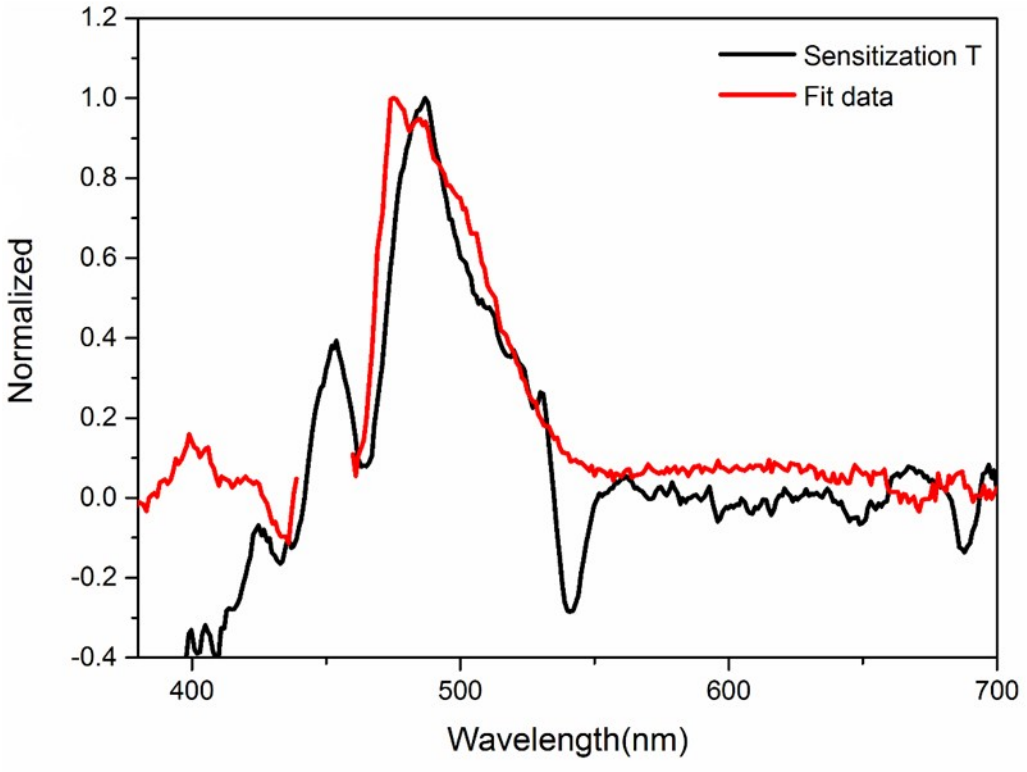

Fig. S8 Comparison of the spectrum of the third component and the T_1state obtained from the sensitization experiment in PhTc-COOH NPs.

12. Comparison of TA spectra and single-wavelength dynamics of PhTc NPs between the raw data and the fitting data with a three-component model obtained from the global analysis

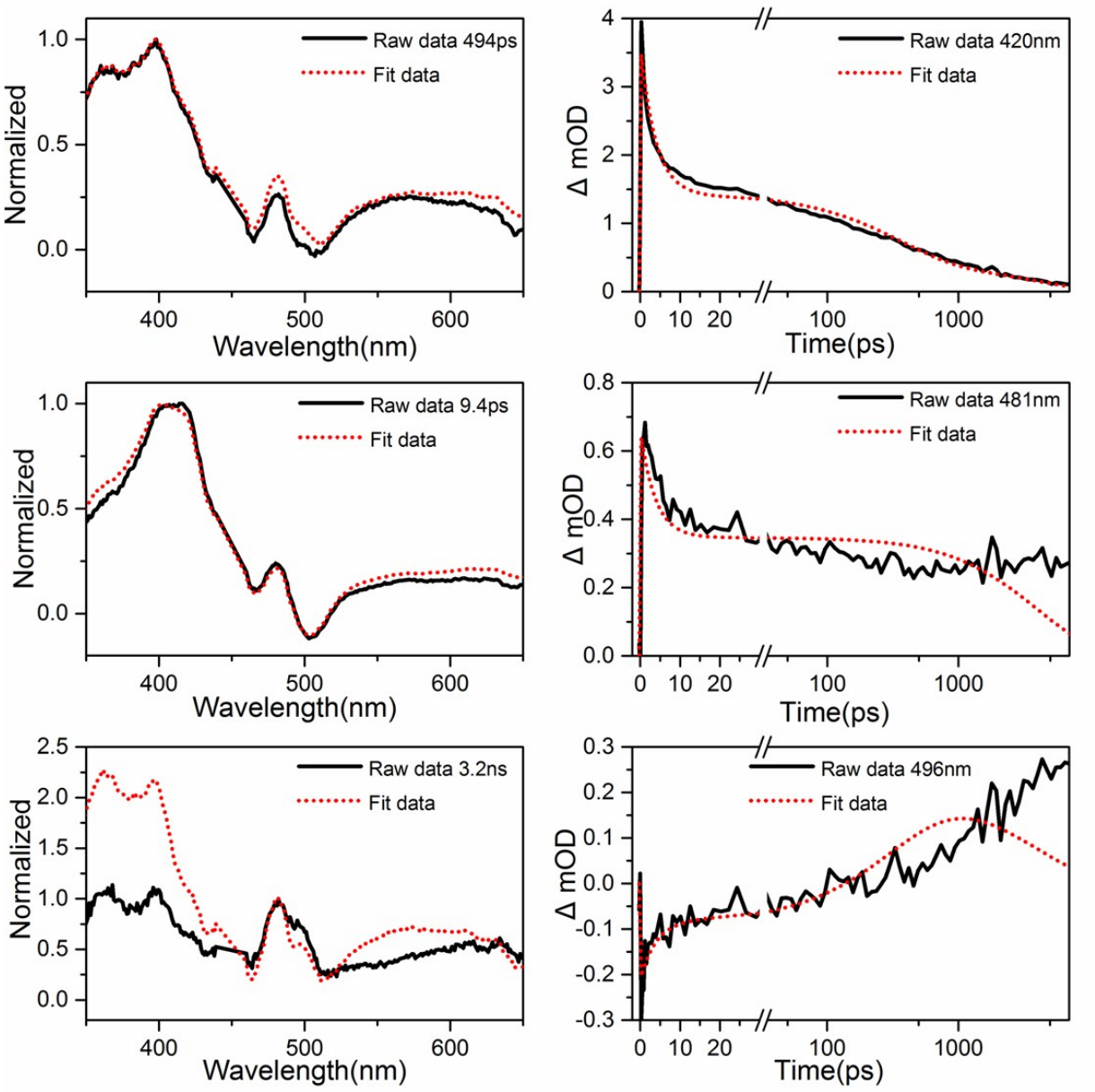

Fig. S9 Comparison of TA spectra and single-wavelength dynamics of PhTc NPs between the raw data and the fitting data with a three-component model obtained from the global analysis.

13. Comparison of TA spectra of PhTc NPs between the raw data and the fitting data in a four-component model obtained from the global analysis

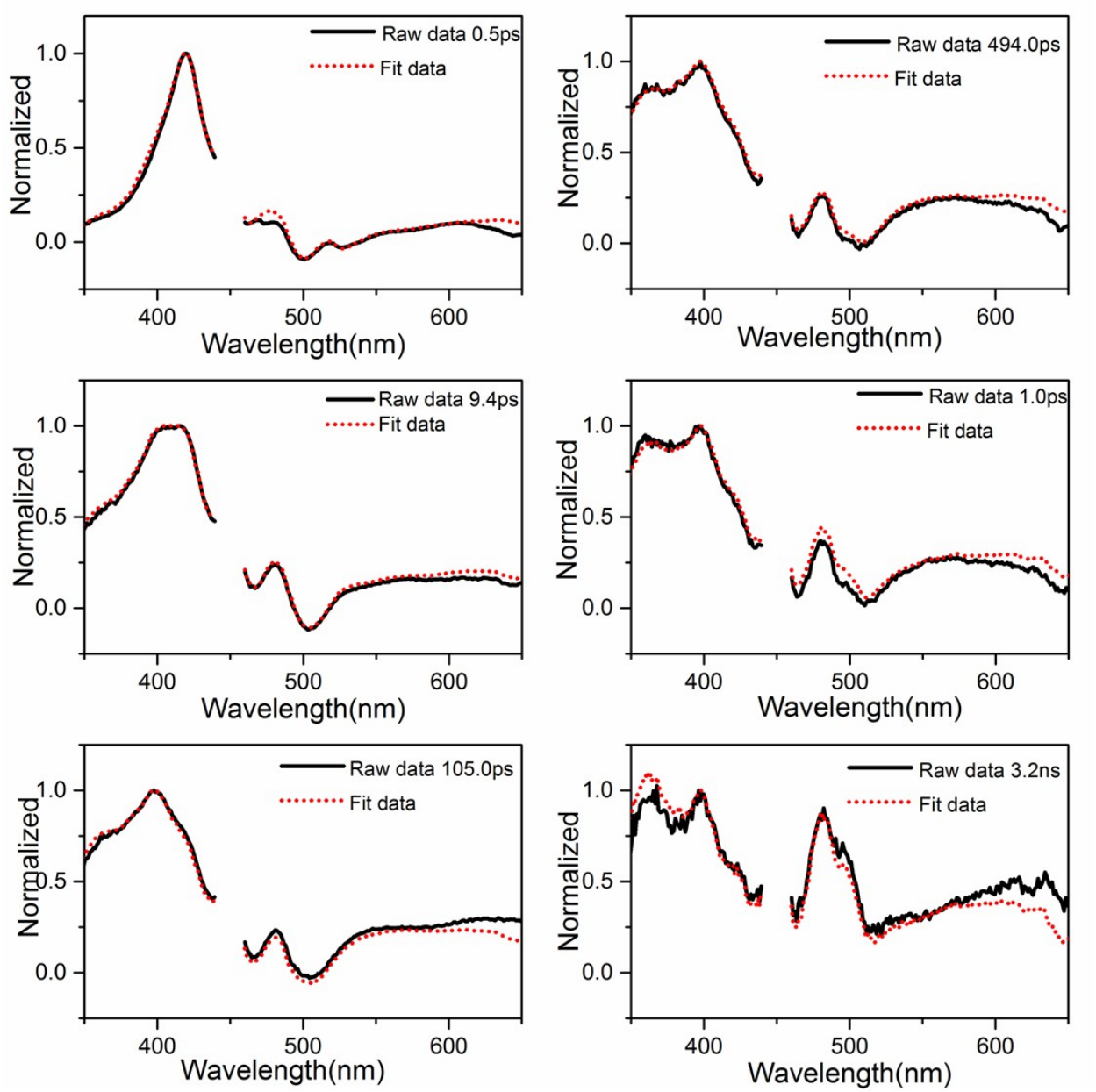

Fig. S10 Comparison of TA spectra of PhTc NPs between the raw data and the fitting data in a four-component model obtained from the global analysis.

14. Comparison of single-wavelength dynamics of PhTc-COOH NPs between the raw data and the fitting data in a four-component model obtained from the global analysis.

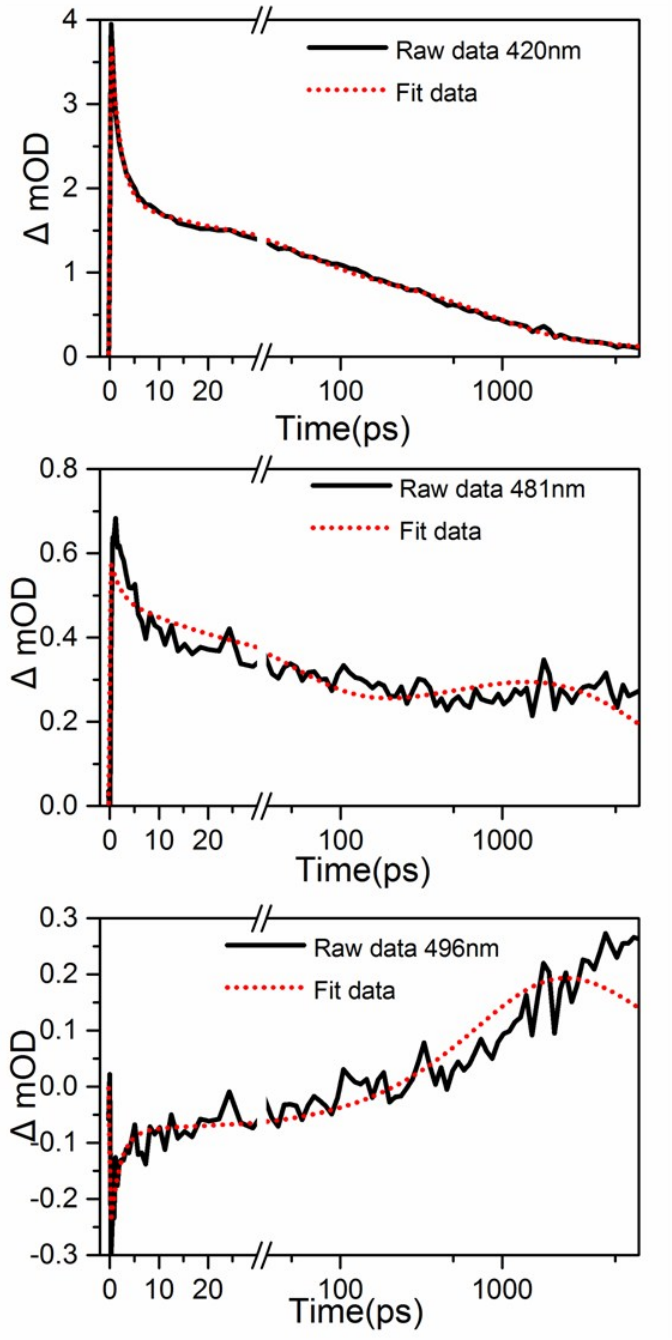

Fig. S11 Comparison of single-wavelength dynamics of PhTc-COOH NPs between the raw data and the fitting data in a four-component model obtained from the global analysis.

15. Triplet yield determination

As the literature report[12,13], an early time trace (0.5ps)after photoexcitation for PhTc-COOH NPs,the S_1 concentration is assumed C_1whereas the T_1 concentration remains nearly 0. At initial time, the S_0 concentration is C_0.

$$\Delta C(0.5\text{ps}) = S_1(0.5\text{ps}) - S_0 = (C_0 - C_1 - 0) - C_0 = -C_1 = -C(S_1) \quad (1)$$

At 1199ps, S_1 depopulates fully as a result of efficient SF and T_1 generates according to the singular value decomposition (SVD).

$$\Delta C(1199\text{ps}) = (C_0 - 0 - C(T_1)) - C_0 = -C(T_1) \quad (2)$$

Therefore, the triplet yield of PhTc-COOH NPs can be obtained from equation 3

$$\Phi_{triplet} = C(T_1)/C(S_1) = -\Delta C(1199\text{ps})/-\Delta C(0.5\text{ps}) = GSB(1199\text{ps})/GSB(0.5\text{ps}) \quad (3)$$

As the same to PhTc-COOH NPs, the triplet yield of PhTc NPscan be obtained from equation 4

$$\Phi_{triplet} = GSB(2288\text{ps})/GSB(0.5\text{ps}) \quad (4)$$

Therefore, the triplet yield is actually propotional to the intensity of the pure GSB as the transient absorption spectra show the superposition of GSB, S_1 absorption or T_1absorption.Thus, proper substration of the scaled GSB spectrum can reproduce the pure S_0, S_1, T_1 spectra and their respective pure GSB. The specific operation is that only enough ground state absorption is added to the transient tracein order toremove the extremum at 493nm, 475nm in PhTc-COOH NPs and 493nm, 481nm in PhTc-COOH NPs due to GSB (Figure S12 and S13). Therefore, the SF

efficiencies and triplet yields can be determined (133 ± 10% for PhTc-COOH NPs, 67 ± 15% for PhTc NPs).

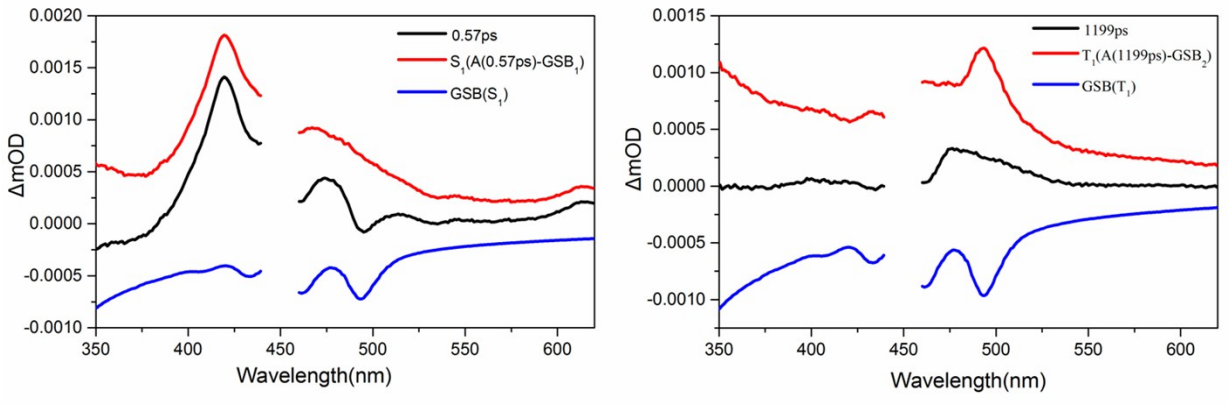

Fig. S12 TA spectra and substration of the scaled steady state absorption spectra and resulting reconstructed absorption spectra of the pure singlet state (left) and triplet state (right) of the PhTc-COOH NPs.

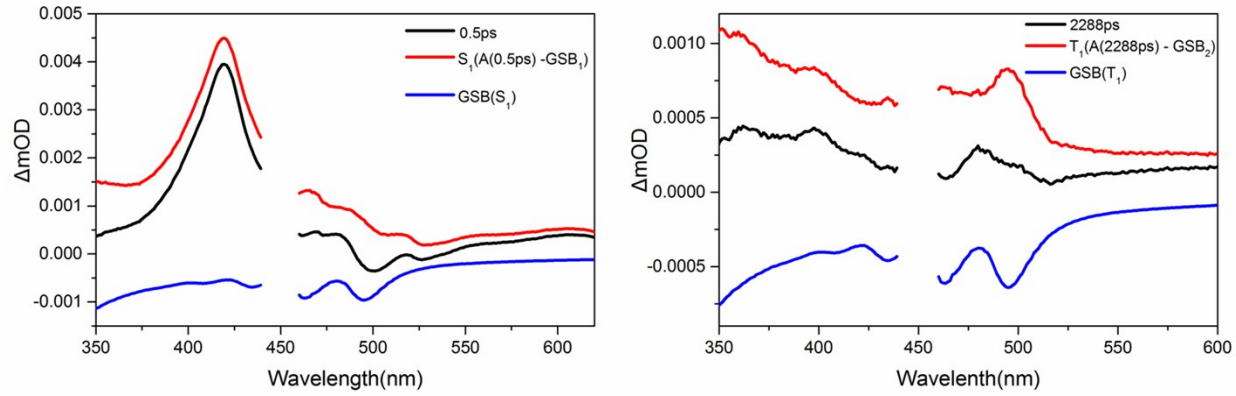

Fig. S13 TA spectra and substration of the scaled steady state absorption spectra and resulting reconstructed absorption spectra of the pure singlet state (left) and triplet state (right) of the PhTc NPs.

16. The 1H NMR spectrum of compound PhTc-COOH.

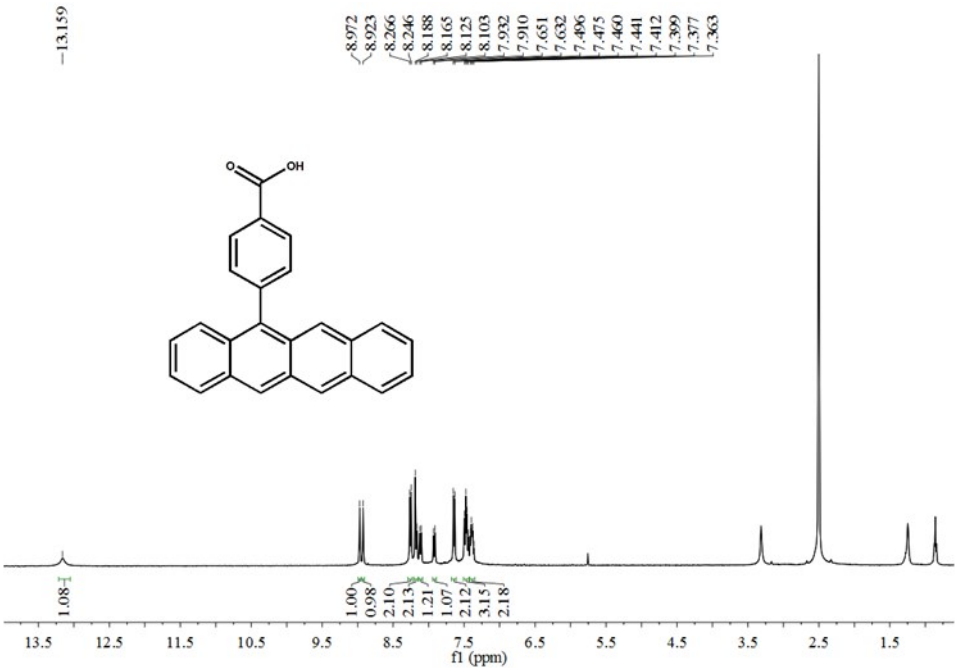

Fig. S14 The ^{1}H NMR spectrum of compound PhTc-COOH.

17. The MALDI-TOF spectrum of compound PhTc-COOH.

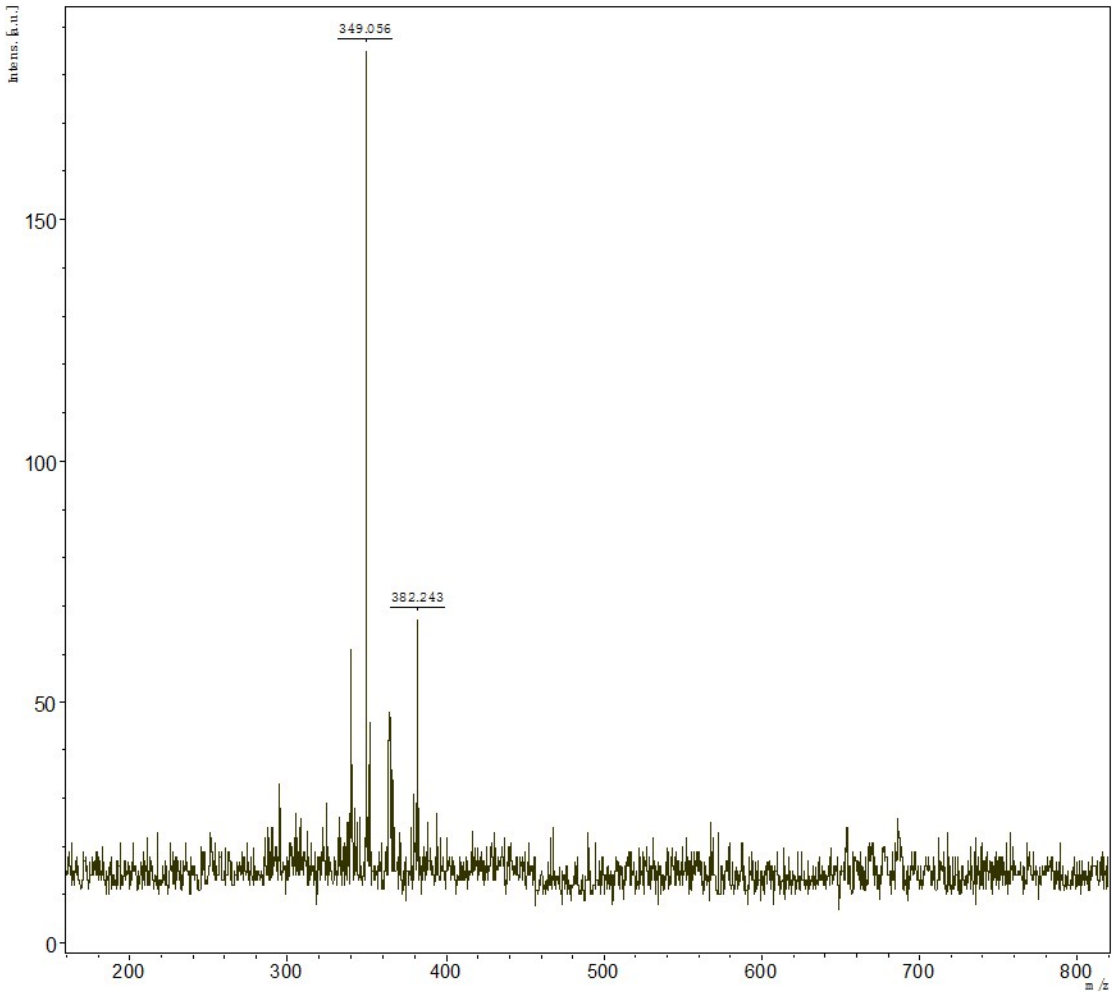

Fig. S15 The MALDI-TOF spectrum of compound PhTc-COOH.

REFERENCES

[1] C. Ming, Yi, C. Yi, L. Yuan, *Chem. Commun.,* 2012, **48**, 12189-12191.

[2] A. M. Müller, Y. S. Avlasevich, W. W. Schoeller, M. Klaus, C. J. Bardeen, *J. Am. Chem. Soc.,* 2007, **129**, 14240-14250.

[3] C. M. Mauck, P. E. Hartnett, Y. L. Wu, C. E. Miller, T. J. Marks, M. R. Wasielewski, *Chem. Mater.,* 2017, **29**, 6810-6817.

[4] R. D. Pensack, C. Grieco, G. E. Purdum, S. M. Mazza, A. J. Tilley, E. E. Ostroumov, D. S. Seferos, Y. L. Loo, J. B. Asbury, J. E. Anthony, *Mater. Horiz.,* 2017, **4**, 915-923.

[5] S. Parkin, H. J. Hope, *App. Crystallogr.,* 1998, **31**, 945-923.

[6] G. M. Sheldrick, *Acta. Crystallogr. C*, A 2015, **71**, 3-8.

[7] H. Liu, Z. Wang, X. Wang, S. Li, C. Zhang, X. Min, X. Li, *J. Mater. Chem. C,* 2018, **6**, 3245-3253.

[8] H. Liu, R. Wang, L. Shen, Y. Xu, M. Xiao, C. Zhang, X. Li, *Org. Lett.,* 2017, **19**, 580-583.

[9] S. T. Roberts, R. E. McAnally, J. N. Mastron, D. H. Webber, M. T. Whited, R. L. Brutchey, M. E. Thompson and S. E. Bradforth, *J. Am. Chem. Soc.,* 2012, **134**, 6388-6400.

[10] J. N. Mastron, S. T. Roberts, R. E. McAnally, M. E. Thompson and S. E. Bradforth, *J. Phys. Chem. A,* 2013, **117**, 15519-15526.

[11] C. Burgdorff, T. Kircher, H. G. Löhmannsröben, *Spectrochim. Acta. A,* 1988, **44**, 1137-1141.

[12] Y. Wu, K. Liu, H. Liu, Y. Zhang, H. Zhang, J. Yao, H. Fu, *J. Phys. Chem. Lett.,* 2014, **5**, 3451-3455.

[13] E. A. Margulies, Y. L. Wu, P. Gawel, S. A. Miller, L. E. Shoer, R. D. Schaller, F. Diederich, M. R. Wasielewski, *Angew. Chem. Int. Ed.,* 2015, **54**, 8679-5683.